symmetry

MDPI

Article

Structural Distortion Stabilizing the Antiferromagnetic and Semiconducting Ground State of BaMn$_2$As$_2$

Ekkehard Krüger

Institut für Materialwissenschaft, Materialphysik, Universität Stuttgart, Stuttgart D-70569, Germany;
ekkehard.krueger@imw.uni-stuttgart.de; Tel.: +49-711-685-61906

Abstract: We report evidence that the experimentally found antiferromagnetic structure as well as the semiconducting ground state of BaMn$_2$As$_2$ are caused by optimally-localized Wannier states of special symmetry existing at the Fermi level of BaMn$_2$As$_2$. In addition, we find that a (small) tetragonal distortion of the crystal is required to stabilize the antiferromagnetic semiconducting state. To our knowledge, this distortion has not yet been established experimentally.

1. Introduction

The electronic ground state of BaMn$_2$As$_2$ shows resemblances but also striking differences, as compared with the ground state of the isostructural compound BaFe$_2$As$_2$. Both materials become antiferromagnetic below the respective Néel temperature. However, while the magnetic moments in BaMn$_2$As$_2$ are orientated along the tetragonal c-axis [1] (see Figure 1), they are orientated perpendicular to this axis in BaFe$_2$As$_2$ [2].
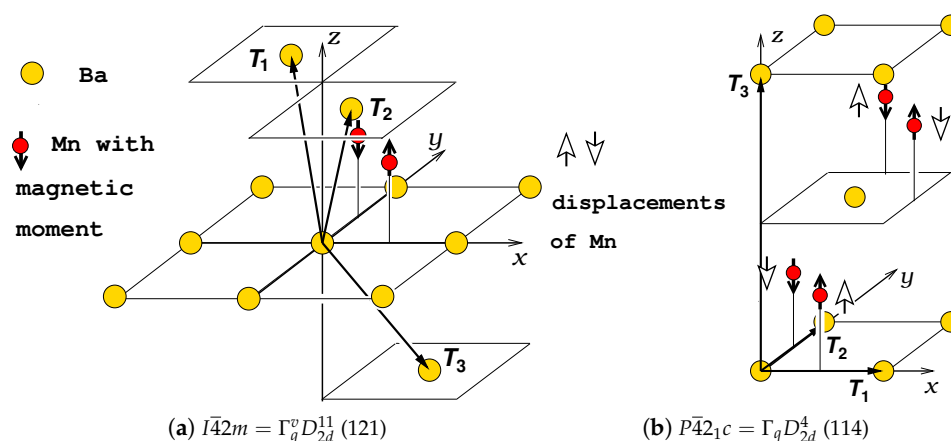

(a) $I\bar{4}2m = \Gamma_q^v D_{2d}^{11}$ (121)   (b) $P\bar{4}2_1c = \Gamma_q D_{2d}^4$ (114)

Figure 1. Experimentally observed [1] antiferromagnetic structure in undistorted (**a**); and distorted (**b**) BaMn$_2$As$_2$. While sufficient Ba atoms are depicted to recognize the orientation of the crystal, the Mn atoms are shown only within the respective unit cell. The As atoms are not included. The indicated (small) displacements of the Mn atoms in exact $\pm T_3$ direction realize the tetragonal primitive space group $P\bar{4}2_1c$. As argued in the text, they are required to stabilize the antiferromagnetic semiconducting state in BaMn$_2$As$_2$.

Also very interesting is the observation that, unlike $BaFe_2As_2$, $BaMn_2As_2$ is a small band gap antiferromagnetic *semiconductor* [3,4]. Calculations of An et al. [3] show that the gap amounts to approximately 0.1 eV. No structural transformation or distortion of $BaMn_2As_2$ in this antiferromagnetic semiconducting state was experimentally detected [1].

The present paper reports evidence that the remarkable features of the electronic ground state of $BaMn_2As_2$ are connected with optimally-localized Wannier functions existing at the Fermi level of $BaMn_2As_2$. These Wannier functions are adapted to the symmetry of the antiferromagnetic structure and constructed from Bloch functions of well-defined symmetry forming narrow "magnetic bands". A precise definition of magnetic bands is given in Ref. [5] (Definition 16 *ibidem*).

The group-theoretical tables, together with the notes to these tables given in the appendix, form the core of the paper. The two tables listing the symmetry labels of all the magnetic bands in undistorted (Table A3) and distorted (Table A6) $BaMn_2As_2$ are the key tables. They are determined following the group-theoretical methods detailed in Ref. [5]. Tables A1, A4 and A7 serve to define the symmetry labels of the representations of the space groups considered in the paper and give the dimension of the irreducible co-representations of the related magnetic groups. Knowledge of this dimension is required to decide whether a magnetic structure with the considered magnetic group may be stable (see Theorem 1 in Ref. [6]). This question, however, is not critical in $BaMn_2As_2$ because all the considered magnetic groups possess suitable co-representations (see Section 2.3). When a band structure in a space group G is folded into the Brillouin zone for a subgroup G' of G, then the symmetry labels of the Bloch functions at the points of symmetry comply with certain compatibility relations. Tables A2 and A5 list the compatibility relations used in this paper. They are determined following the methods detailed in Ref. [7].

In Section 2.1, we shall identify the tetragonal space group $I\bar{4}2m$ (121) as the space group of the antiferromagnetic structure observed in $BaMn_2As_2$ (the number in parenthesis is the international number) and determine the magnetic group M_{121} of this structure. We will show that no magnetic band related to M_{121} exists in the band structure of $BaMn_2As_2$. The situation changes drastically when in Section 2.2, we shall consider a slightly distorted crystal. We will define and verify the existence of a magnetic "super" band in distorted antiferromagnetic $BaMn_2As_2$. This super band consists of three magnetic bands with Wannier functions situated at the Ba, the Mn, and the As atoms, respectively.

Our group-theoretical results in Section 2 will be physically interpreted in Section 3. We will argue in Section 3.1 that a small tetragonal distortion of the crystal is required to stabilize the antiferromagnetic semiconducting ground state of $BaMn_2As_2$. This distortion alters the space group $I\bar{4}2m = \Gamma_q^v D_{2d}^{11}$ of the undistorted antiferromagnetic crystal into the space group $P\bar{4}2_1c = \Gamma_q D_{2d}^4$ (which is still tetragonal) and may be realized by the displacements of the Mn atoms depicted in Figure 1b. These displacements are evidently so small that they have not yet been experimentally verified [1]. In Section 3.2, we shall show that evidently the magnetic super band is responsible for the small band gap in the antiferromagnetic semiconducting ground state, and, in Section 3.3, why the space groups of the magnetic structures in $BaFe_2As_2$ and $BaMn_2As_2$ differ so strikingly.

1.1. Nonadiabatic Heisenberg Model

The existence of magnetic bands in the band structure of $BaMn_2As_2$ is physically interpreted within the nonadiabatic Heisenberg model (NHM) [8]. The second postulate of the NHM (Equation (2.19) of [8]) states that, in narrow bands, the electrons may lower their total correlation energy by condensing into an atomic-like state, as it was described by Mott [9] and Hubbard [10]: the electrons occupy the localized states as long as possible and perform their band motion by hopping from one atom to another. Within the NHM, however, the localized states *are not represented by (hybrid) atomic orbitals but consequently by symmetry-adapted optimally-localized Wannier states*. In contrast to atomic functions, Wannier functions situated at adjacent atoms are orthogonal and form a complete set of basis functions within the considered narrow, partially filled band. Consequently, Wannier functions contain all the physical information about the band.

In the atomic-like state, the electrons are strongly correlated, leading to the consequence that a consistent description of the localized Wannier states must involve the nonadiabatic motion of the atomic cores. Hence, the nonadiabatic localized functions representing these nonadiabatic Wannier states depend on an additional coordinate characterizing the motion of the atomic cores. Fortunately, these mathematically complicated functions need not be explicitly known. They can be simply managed within the group-theoretical NHM because they have the same symmetry as the related adiabatic optimally-localized Wannier functions. In this context, we speak of "adiabatic" Wannier functions if they do not depend on the nonadiabatic motion of the atomic cores.

At the transition from an adiabatic band-like motion of the electrons into the nonadiabatic atomic-like state, the total Coulomb energy of the electron system decreases by the nonadiabatic condensation energy ΔE defined in Equation (2.20) of [8].

2. Magnetic Bands in the Band Structure of BaMn$_2$As$_2$

2.1. The Space Group $I\bar{4}2m$ (121) of the Antiferromagnetic Structure in Undistorted BaMn$_2$As$_2$

The space group $I4/mmm$ of paramagnetic BaMn$_2$As$_2$ [1] contains symmetry operations not leaving invariant the antiferromagnetic structure. Removing these symmetry operations from $I4/mmm$, we obtain the space group $I\bar{4}2m$ (121) of undistorted antiferromagnetic BaMn$_2$As$_2$. Just as $I4/mmm$, the group $I\bar{4}2m$ has the tetragonal body-centered Bravais lattice Γ_q^v.

The group $I\bar{4}2m$ may be defined by the two "generating elements"

$$\{S_{4z}^+|000\} \text{ and } \{C_{2x}|000\} \tag{1}$$

(see Table 3.7 of Ref. [11]). Just as in all of our papers, we write the symmetry operations $\{R|pqr\}$ in the Seitz notation detailed in the textbook of Bradley and Cracknell [11]: R stands for a point group operation (as defined, e.g., in Table 1.4 *ibidem*) and pqr denotes the subsequent translation $t = pT_1 + qT_2 + rT_3$, where the T_1, T_2 and T_3 denote the basic vectors of the respective Bravais lattice given in Figure 1. A (magnetic) structure is invariant under a space group G if it is already invariant under the generating elements of G. The two generating symmetry operations (1) leave invariant the atoms of BaMn$_2$As$_2$ since both operations are elements of $I4/mmm$. By means of Figure 1a, we can realize that they additionally leave invariant the magnetic structure, cf. Section 3.1 of Ref. [12].

The associated magnetic group reads as

$$M_{121} = I\bar{4}2m + \{KI|000\}I\bar{4}2m \tag{2}$$

where K and I denote the operator of time inversion and the inversion, respectively. $\{KI|000\}$ leaves invariant both the atoms and the magnetic structure since $\{I|000\} \in I4/mmm$.

With consideration of the change of symmetry by the magnetostriction, but neglecting all other magnetic interactions, we receive from the band structure of BaMn$_2$As$_2$ given in Figure 2 the band structure of antiferromagnetic undistorted BaMn$_2$As$_2$ depicted in Figure 3. All the possible magnetic bands (Definition 16 of Ref. [5]) in the magnetic group M_{121} are listed in Table A3. The "best" magnetic band would be band 2 of Mn as highlighted in Figure 3 by the red labels.

Band 2 of Mn, however, is not a magnetic band in BaMn$_2$As$_2$ because it misrepresents the Bloch functions at parts of the Fermi level. Between the N_1 and P_3 states, it jumps over the Fermi level simulating in this way Bloch states at the Fermi level that do not exist. We have the same situation between the Z_5 state and the two X_3, X_1 states. Along the lines F, Σ, the Γ_5 state is connected with two Bloch states at the Fermi level, which, however, are not connected to Z_5.
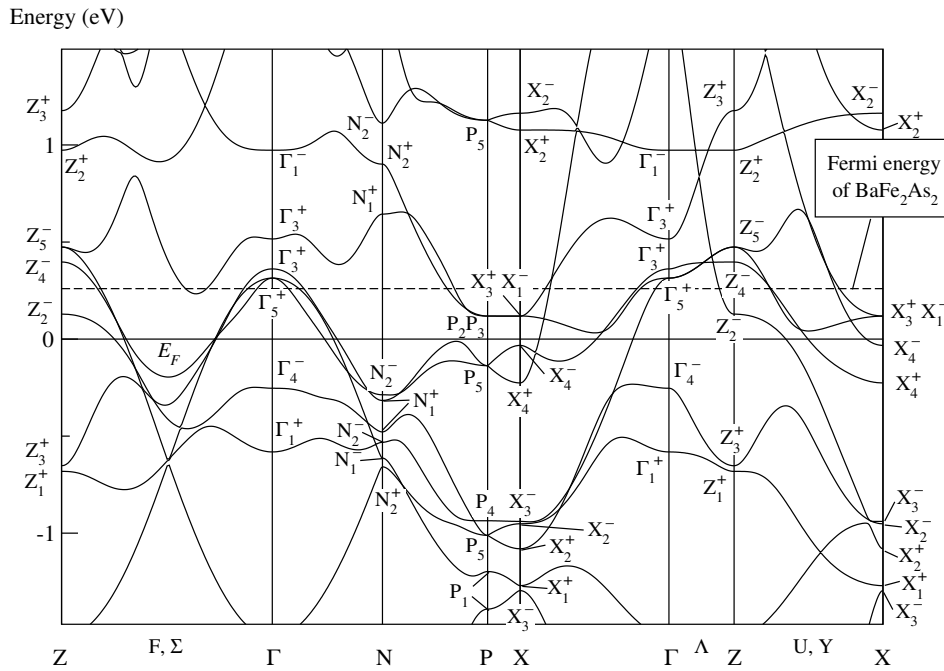
Figure 2. Band structure of BaMn$_2$As$_2$ as calculated by the "Fritz Haber Institute ab initio molecular simulations" (FHI-aims) program [13,14], using the structure parameters given in Ref. [1]. The space group of BaMn$_2$As$_2$ is the tetragonal group $I4/mmm$ (139) [1], the given symmetry labels are determined by the author. The notations of the points and lines of symmetry in the Brillouin zone for Γ_q^v follow Figure 3.10b of Ref. [11], and the symmetry labels are defined in Table 2 of Ref. [6]. E_F denotes the Fermi level. The band structure of BaMn$_2$As$_2$ essentially coincides with the band structure of BaFe$_2$As$_2$ (depicted in Figure 2 of Ref. [6]) when the Fermi level is moved upwards to the dashed line.
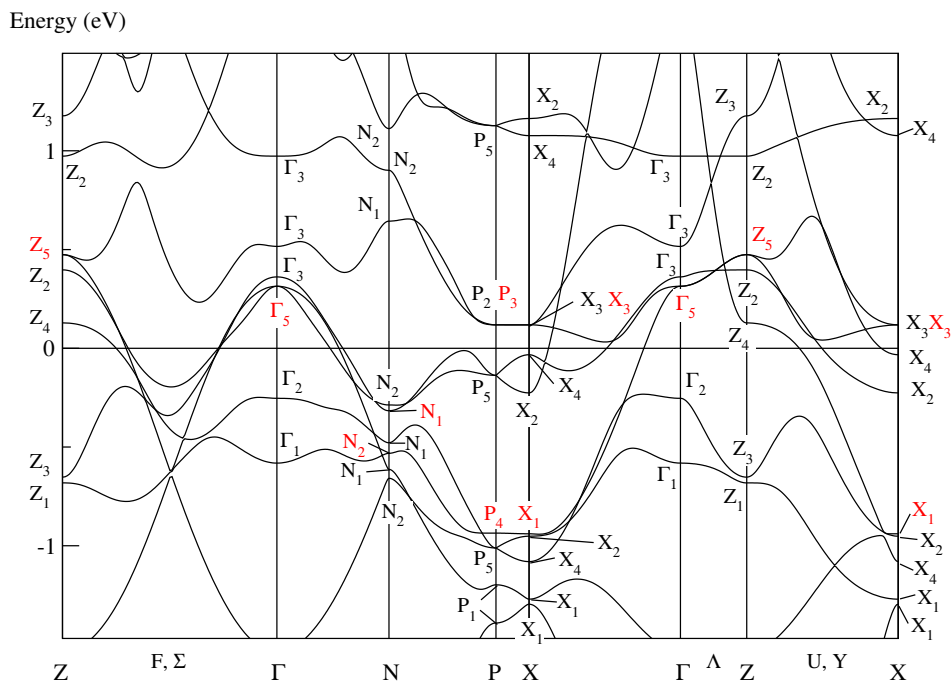
Figure 3. Band structure of BaMn$_2$As$_2$ as given in Figure 2 with symmetry labels of the space group $I\bar{4}2m$ (121) of the antiferromagnetic structure in undistorted BaMn$_2$As$_2$. The symmetry labels are determined from Table A2. The labels highlighted in **red** define band 2 of Mn in Table A3.

We could try to render ineffective these unfavorable jumps by adding further bands to the Mn band, as it will be successful in the space group $P\bar{4}2_1c$ considered in the following Section 2.2. By means of Table A3, we may satisfy ourselves that this procedure is not possible. For instance, we neither can add band 1 nor band 2 of As to band 2 of Mn because there is neither a Γ_4 state nor an additional P_3 state available in the band structure.

2.2. The Space Group $P\bar{4}2_1c$ (114) of the Antiferromagnetic Structure in Distorted BaMn$_2$As$_2$

The situation described in the preceding Section 2.1 changes drastically when we consider the space group $P\bar{4}2_1c$. This group no longer has the tetragonal body-centered Bravais lattice Γ_q^v, but the tetragonal primitive lattice Γ_q and may be defined by the two generating elements

$$\{S_{4z}^+|000\} \text{ and } \{C_{2x}|\tfrac{1}{2}\tfrac{1}{2}\tfrac{1}{2}\} \tag{3}$$

(see Table 3.7 of Ref. [11] (note that the basis vectors now are given in Figure 1b)). As well as the generating elements of $I\bar{4}2m$ (1), they leave invariant both the positions of the atoms and the magnetic structure since the vector $\boldsymbol{t} = (\tfrac{1}{2}\tfrac{1}{2}\tfrac{1}{2})$ is a lattice vector in Γ_q^v. In addition, the generating elements (3) leave invariant the displacements of the Mn atoms depicted in Figure 1b. Thus, these displacements "realize" the space group $P\bar{4}2_1c$ in the sense that the electrons now move in a potential adapted to the symmetry of the distorted crystal. The group $P\bar{4}2_1c$ represents only a small distortion of the crystal because it is still tetragonal and possesses the same point group as the space group $I\bar{4}2m$ of antiferromagnetic undistorted BaMn$_2$As$_2$. It is only the translation $\boldsymbol{t} = (\tfrac{1}{2}\tfrac{1}{2}\tfrac{1}{2})$ that is no longer a symmetry operation in $P\bar{4}2_1c$.

At first, the two anti-unitary operations $\{KI|000\}$ and $\{KI|\tfrac{1}{2}\tfrac{1}{2}\tfrac{1}{2}\}$ may define the magnetic group of the magnetic structure since both operations leave invariant the magnetic structure. However, only $\{KI|\tfrac{1}{2}\tfrac{1}{2}\tfrac{1}{2}\}$ leaves additionally invariant the displacement of the Mn atoms depicted in Figure 1b. These displacements, however, are required to realize the space group $P\bar{4}2_1c$. Hence, the magnetic group of antiferromagnetic distorted BaMn$_2$As$_2$ may be written as

$$M_{114} = P\bar{4}2_1c + \{KI|\tfrac{1}{2}\tfrac{1}{2}\tfrac{1}{2}\}P\bar{4}2_1c. \tag{4}$$

Folding the band structure of BaMn$_2$As$_2$ as given in Figure 2 into the Brillouin zone for $P\bar{4}2_1c$, we receive the band structure depicted in Figure 4. All the magnetic bands in the magnetic group M_{114} are listed in Table A6. Now, we have a very interesting situation not yet considered in our former papers: we are able to assign optimally-localized symmetry-adapted Wannier functions to all the atoms in the unit cell of Γ_q, meaning that we have a band of ten branches with Wannier functions at the two Ba, the four Mn and the four As atoms. Such a magnetic band related to all the atoms in the unit cell we call magnetic "super" band. It is highlighted in red in Figure 4 and consists of band 1 of Mn, band 2 of As and band 3 of Ba in Table A6 and, hence, is defined by the symmetry labels

$$
\begin{aligned}
&\Gamma_1, \Gamma_2, \Gamma_3, \Gamma_4, \quad && 2\Gamma_5, \quad && \Gamma_3, \Gamma_4, \\
&M_1, M_2, M_3, M_4, \quad && M_1, M_2, M_3, M_4, \quad && M_5, \\
&2Z_5, \quad && Z_1, Z_2, Z_3, Z_4, \quad && Z_5, \\
&2A_5, \quad && 2A_5, \quad && A_1, A_2, \\
&2R_1, \quad && 2R_1, \quad && R_1, \\
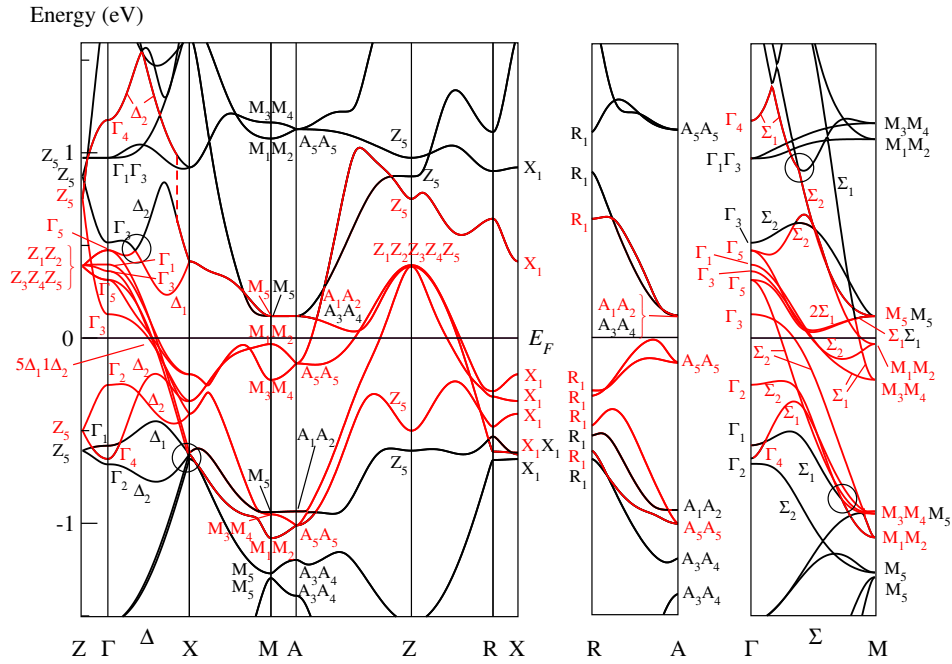&2X_1, \quad && 2X_1, \quad && X_1.
\end{aligned}
\tag{5}
$$

Figure 4. The band structure of BaMn$_2$As$_2$ as given in Figure 2 folded into the Brillouin zone for the tetragonal primitive Bravais lattice Γ_q of the space group $P\bar{4}2_1c$ (114). The symmetry labels are defined in Table A4 and are determined from Figure 2 by means of Table A5. The notations of the points of symmetry follow Figure 3.9 of Ref. [11]. E_F denotes the Fermi level. The lines and symmetry labels highlighted in **red** form the magnetic "super" band of the experimentally observed [1] antiferromagnetic structure in BaMn$_2$As$_2$. Whenever a **black** and a **red** line overlap, the **red** line lies on the top.

While the magnetic super band in BaMn$_2$As$_2$ satisfies the condition (38) of Theorem 5 of Ref. [5] at all the points of symmetry, there are few complications on the lines Σ and Δ in two branches: The four circles in Figure 4 mark regions with unavoidable transitions from Δ_2 to Δ_1, Δ_1 to Δ_2, Σ_1 to Σ_2, and Σ_2 to Σ_1 symmetry. These transitions clearly destroy the $P\bar{4}2_1c$ symmetry of the Wannier functions. However, since these transitions only occur in two lines of two branches far away from the Fermi level, we assume that the magnetic structure of BaMn$_2$As$_2$ may be described with high accuracy in the space group $P\bar{4}2_1c$. Nevertheless, these transitions produce an additional small distortion of the crystal going beyond the displacements of the Mn atoms depicted in Figure 1b. This additional small distortion is not considered in this paper. However, we should keep in mind (see Note (v) of Table A7) that the Wannier functions are *exactly* adapted to the space group $P\bar{4} = \Gamma_q S_4^1$ (81) since, in this space group, the mentioned complications on the lines Σ and Δ disappear. The related exact magnetic group is a subgroup of M_{114} (4). First, there exist two subgroups of M_{114} defined by the two anti-unitary operations $\{KC_{2a}|000\}$ and $\{KI|\frac{1}{2}\frac{1}{2}\frac{1}{2}\}$, respectively. A detailed examination shows that only the group

$$M_{81} = P\bar{4} + \{KC_{2a}|000\}P\bar{4} \tag{6}$$

allows an additional distortion of the crystal.

2.3. Time-Inversion Symmetry

The time-inversion symmetry is no essential object in antiferromagnetic BaMn$_2$As$_2$: all three of the space groups $I\bar{4}2m$ (121), $P\bar{4}2_1c$ (114), and $P\bar{4}$ (81) possess one-dimensional representations allowing a *stable* magnetic state with the magnetic group M_{121} (2), M_{114} (4), and M_{81} (6), respectively (see Tables A1, A4 and A7 and the notes to these tables). Consequently, time-inversion symmetry influences neither the antiferromagnetic structure nor the structural distortions in BaMn$_2$As$_2$ (as it

is the case, for instance, in $BaFe_2As_2$ [6]). Time-inversion symmetry only forbids magnetic moments located at the As atoms (see Note (x) of Table A6).

3. Physical Interpretation

The existence and the properties of the roughly half-filled magnetic super band in the band structure of $BaMn_2As_2$ yield to an understanding of three phenomena that shall be considered in this section:

- the experimentally observed [1] antiferromagnetic order together with a structural distortion not yet experimentally found;
- the semiconducting ground state; and
- the different magnetic structures in $BaMn_2As_2$ and $BaFe_2As_2$.

3.1. The Antiferromagnetic Order and the Structural Distortion in $BaMn_2As_2$

In a material possessing a narrow, roughly half-filled magnetic band or super band related to a magnetic group M, the NHM defines a nonadiabatic Hamiltonian H^n representing atomic-like electrons (Section 1.1) within this band [8]. An important feature of H^n is that it only commutes with the symmetry operations of M, but *does not commute* with the remaining symmetry operations of the paramagnetic group of the crystal. This follows from the fact that the optimally-localized Wannier functions in a magnetic band may be chosen symmetry-adapted to M, but cannot be chosen symmetry-adapted to the complete paramagnetic group (see the detailed discussion of this problem in the introduction of Ref. [5]).

Hence, the electrons in such a narrow, roughly half-filled magnetic band or super band may condense into an atomic-like state only if the electrons really move in a potential with the magnetic group M. Thus, the electrons may gain the nonadiabatic condensation energy ΔE (Section 1.1) *only if a magnetic structure with the magnetic group M really exists*. As a consequence, the electrons *activate* in the nonadiabatic system a spin dependent exchange mechanism producing a magnetic structure with the magnetic group M [15,16].

In the case of $BaMn_2As_2$, the group $I\bar{4}2m$ (121) is the space group of the antiferromagnetic structure in *undistorted* $BaMn_2As_2$. However, within this group, there does not exist a magnetic band (see Section 2.1). Indeed, a magnetic band, even a magnetic super band, exists in the space group $P\bar{4}2_1c$ (114) of distorted $BaMn_2As_2$ (see Section 2.2).

Hence, in $BaMn_2As_2$, the electron system cannot condense into the atomic-like state by the production of the magnetic structure *alone* but must additionally produce a spatial distortion of the crystal realizing—together with the magnetic structure—the magnetic group M_{114} (4). By "realize," we mean that this distortion

(i)   no longer possesses the space group $I\bar{4}2m$;
(ii)   but is invariant under the space group $P\bar{4}2_1c$ and, additionally,
(iii)   is invariant under the anti-unitary operation $\{KI|\frac{1}{2}\frac{1}{2}\frac{1}{2}\}$ defining the magnetic group M_{114} (4).

This is achieved by the displacements of the Mn atoms depicted in Figure 1b. These displacements of the Mn atoms in opposite direction to each other form the only distortion realizing the magnetic group M_{114} (4). Displacements in the same direction, for instance, neither are invariant under the space group $I\bar{4}2m$ nor under $P\bar{4}2_1c$. Each displacement of the As atoms is either invariant under the full space group $I\bar{4}2m$ or it is not invariant under both $I\bar{4}2m$ and $P\bar{4}2_1c$; and no displacement of the Ba atoms is possible in the space group $P\bar{4}2_1c$.

Consequently, the magnetically ordered ground state of $BaMn_2As_2$ is accompanied by the displacements of the Mn atoms depicted in Figure 1b. With our group-theoretical methods, however, we cannot determine the size of these displacements. Likely, they have the same order of magnitude as the displacements of the Fe and O atoms in LaOFeAs as established by the excellent neutron diffraction

experiments of Clarina de la Cruz et al. [17]. Evidently, these displacements in LaOFeAs exist because the magnetic group of the *undistorted* crystal does not possess suitable co-representations [6].

3.2. The Semiconducting Ground State of $BaMn_2As_2$

The magnetic super band defines not only Wannier functions situated at *all the* atoms of $BaMn_2As_2$, but it also comprises *all the Bloch states* at the Fermi level (see Figure 4). Thus, if the magnetic super band is *exactly* half filled, the nonadiabatic Hamiltonian H^n produces very specific atomic-like electrons: at *any* atom of $BaMn_2As_2$, there exists a localized Wannier state occupied by exactly one electron, and, besides these atomic-like electrons, there do not exist band-like electrons that would be able to transport electrical current. Thus, H^n possesses a semiconducting ground state since the atomic-like state is separated from any band-like state by the nonadiabatic condensation energy ΔE mentioned in Section 1.1. The experimental observation of an insulating ground state in $BaMn_2As_2$ suggests that, indeed, the magnetic super band is exactly half-filled.

3.3. Different Magnetic Structures in $BaMn_2As_2$ and $BaFe_2As_2$

While both compounds $BaMn_2As_2$ and $BaFe_2As_2$ exhibit an antiferromagnetic ordering below the respective Néel temperature, the space groups of the magnetic structures are quite different: in $BaMn_2As_2$, the space group of the magnetic structure is the tetragonal group $P\bar{4}2_1c$ (114) with magnetic moments oriented along the tetragonal c-axis, and, in $BaFe_2As_2$, it is the orthorhombic group *Cmca* with magnetic moments orientated perpendicular to the c-axis (see Figure 1 of [1] and Figure 3 of [2], respectively).

This surprising experimental observation can be understood comparing the band structures of both compounds as given in Figure 2 and Figure 2 of Ref. [6]. The band structure of $BaFe_2As_2$ is very similar to the band structure of $BaMn_2As_2$. The essential difference is the position of the Fermi level, as mainly caused by the one additional electron in $BaFe_2As_2$: we may approximate the band structure of $BaFe_2As_2$ by the band structure of $BaMn_2As_2$ by shifting the Fermi level upwards by about 0.3 eV, as it is indicated in Figure 2.

A magnetic (super) band may be physically active only if the band is nearly half-filled. The band width of the (red) magnetic super band in Figure 4 may be approximated by 2σ, where

$$\sigma = \sqrt{\frac{1}{N}\sum_{k}(E_k - E_F)^2} \approx 0.5\text{eV} \tag{7}$$

denotes the standard deviation of the $N = 6 \times 10$ energy values E_k in the six points of symmetry of the magnetic super band.

Thus, the Fermi level is shifted in $BaFe_2As_2$ nearly to the top of the magnetic super band. Hence, in $BaFe_2As_2$, this band is far from being half-filled and determines neither the magnetic structure nor produces an isolating ground state in $BaFe_2As_2$. Instead, the magnetic structure in $BaFe_2As_2$ is determined by the nearly half-filled magnetic band presented in Figure 3 of Ref. [6], which is related to the space group *Cmca* of the magnetic structure experimentally found in $BaFe_2As_2$ [2].

3.4. Discussion

As stated in Section 1.1, the NHM starts from the symmetry of the best localized *nonadiabatic* Wannier functions representing the magnetic super band, and considers in this way the *true* atomic-like motion in the nonadiabatic electron system. By "true," we mean that no simplifying assumptions in respect of the electronic motion were made. On this basis, the NHM gives clear group-theoretical statements on which magnetic structure may be realized and which structural distortions are required to stabilize this structure. In addition, it may predict a small band gap semiconducting ground state. This can be compared with the selection rules in atomic physics. Here, group theory does not make

statements on the physical nature of the atomic transitions, but only states which transitions are allowed and which are not.

Likewise, the group-theoretical NHM has clear limits: it does not provide any method to calculate the exchange couplings responsible for the magnetic structure, the value of the magnetic moments, the size of the displacements of the Mn atoms, or the value of the band gap. These limitations are due to the fact that the highly complex nonadiabatic Wannier functions are, apart from their symmetry, unknown. A basis for an understanding of the nature of the exchange mechanism still are (hybrid) atomic functions. I believe that the selection of the optimal atomic basis in the Heisenberg model will be affected by the NHM. Nevertheless, the exchange mechanism activated within the NHM in $BaMn_2As_2$ and $BaFe_2As_2$ should largely coincide with the mechanism described by Singh et al. [1], according to which the magnetic structure in $BaMn_2As_2$ is produced by exchange interaction among nearest neighbors, while, in $BaFe_2As_2$, it is also produced by a strong coupling among next-nearest neighbors.

The electrons in the magnetic super band may lower their total Coulomb energy by condensing into the *strongly correlated* atomic-like state, which is represented by the nonadiabatic Wannier functions. In this way, the electron system gains the nonadiabatic condensation energy ΔE. Thus, the phenomena discussed in this section are caused by strongly correlated electrons and cannot be directly observed in the band structure. The band structure only provides the symmetry of the Bloch functions that defines the symmetry of the nonadiabatic Wannier functions.

4. Conclusions

This paper emphasizes the importance of the nonadiabatic condensation energy ΔE defined in Equation (2.20) of Ref. [8] (and already mentioned in Section 1.1), which is evidently responsible for the striking electronic features of $BaMn_2As_2$. ΔE is released at the transition from an adiabatic band-like motion of the electrons to the nonadiabatic strongly-correlated atomic-like motion.

This finding is in accordance with former observations on a great number of superconducting and magnetic materials (see Section 1 of [5]), suggesting that superconductivity and magnetism are always connected with superconducting (Definition 22 of Ref. [5]) and magnetic bands, respectively. Thus, in superconducting and magnetic bands, the nonadiabatic condensation energy ΔE may evidently produce superconductivity and magnetism, respectively, and, in some cases, even a small band gap semiconductor.

Conflicts of Interest: The author declares no conflict of interest.

Appendix A. Group-Theoretical Tables

This appendix provides Tables A1–A7 along with notes to the tables.

Table A1. Character tables of the irreducible representations of the tetragonal space group $I\bar{4}2m = \Gamma_q^v D_{2d}^{11}$ (121) of the experimentally observed [1] antiferromagnetic structure in $BaMn_2As_2$.

$\Gamma(000), Z(\frac{1}{2}\frac{1}{2}\bar{\frac{1}{2}})$										$P(\frac{1}{4}\frac{1}{4}\frac{1}{4})$							
					S_{4z}^-	C_{2y}	σ_{da}							S_{4z}^-	C_{2y}	σ_{da}
	K	KI	E	C_{2z}	S_{4z}^+	C_{2x}	σ_{db}		K	KI	E	C_{2z}	S_{4z}^+	C_{2x}	σ_{db}
Γ_1, Z_1	(a)	(a)	1	1	1	1	1	P_1	(x)	(a)	1	1	1	1	1
Γ_2, Z_2	(a)	(a)	1	1	1	−1	−1	P_2	(x)	(a)	1	1	1	−1	−1
Γ_3, Z_3	(a)	(a)	1	1	−1	1	−1	P_3	(x)	(a)	1	1	−1	1	−1
Γ_4, Z_4	(a)	(a)	1	1	−1	−1	1	P_4	(x)	(a)	1	1	−1	−1	1
Γ_5, Z_5	(a)	(a)	2	−2	0	0	0	P_5	(x)	(a)	2	−2	0	0	0

Table A1. *Cont.*

$X(00\frac{1}{2})$					$N(0\frac{1}{2}0)$		
	E	C_{2z}	σ_{db}	σ_{da}		E	C_{2y}
X_1	1	1	1	1	N_1	1	1
X_3	1	1	-1	-1	N_2	1	-1
X_2	1	-1	1	-1			
X_4	1	-1	-1	1			

Notes to Table A1

(i)   The notations of the points of symmetry follow Figure 3.10b of Ref. [11].
(ii)   The character tables are determined from Table 5.7 of Ref. [11].
(iii)   *K* denotes the operator of time inversion. The entry (a) indicates that the related co-representations of the magnetic groups $I\bar{4}2m + \{K|000\}I\bar{4}2m$ and $I\bar{4}2m + \{KI|000\}I\bar{4}2m$ follow case (a) as defined in Equation (7.3.45) of Ref. [11] (and determined by Equation (7.3.51) of Ref. [11]). This information is interesting only in symmetry points invariant under the complete space group. (x) indicates that *K* does not leave invariant the point *P*.
(iv)   The one-dimensional representations at point *P* would be possible representations of a stable antiferromagnetic state because they comply with the demands in Section III C of Ref. [15].

Table A2. Compatibility relations between the Brillouin zone for the space group $I4/mmm$ (139) of paramagnetic BaMn$_2$As$_2$ and the Brillouin zone for the space group $I\bar{4}2m$ (121) of the antiferromagnetic structure in undistorted BaMn$_2$As$_2$.

$\Gamma(000)$										$N(0\frac{1}{2}0)$			
Γ_1^+	Γ_2^+	Γ_3^+	Γ_4^+	Γ_5^+	Γ_1^-	Γ_2^-	Γ_3^-	Γ_4^-	Γ_5^-	N_1^+	N_1^-	N_2^+	N_2^-
Γ_1	Γ_2	Γ_3	Γ_4	Γ_5	Γ_3	Γ_4	Γ_1	Γ_2	Γ_5	N_1	N_1	N_2	N_2

$X(00\frac{1}{2})$							
X_1^+	X_2^+	X_3^+	X_4^+	X_1^-	X_2^-	X_3^-	X_4^-
X_1	X_4	X_3	X_2	X_3	X_2	X_1	X_4

$Z(\frac{1}{2}\frac{1}{2}\bar{\frac{1}{2}})$										$P(\frac{1}{4}\frac{1}{4}\frac{1}{4})$				
Z_1^+	Z_2^+	Z_3^+	Z_4^+	Z_5^+	Z_1^-	Z_2^-	Z_3^-	Z_4^-	Z_5^-	P_1	P_2	P_3	P_4	P_5
Z_1	Z_2	Z_3	Z_4	Z_5	Z_3	Z_4	Z_1	Z_2	Z_5	P_1	P_2	P_3	P_4	P_5

Notes to Table A2

(i)   The Brillouin zone for $I\bar{4}2m$ is identical to the Brillouin zone for $I4/mmm$.
(ii)   The upper rows list the representations of the little groups of the points of symmetry in the Brillouin zone for $I4/mmm$. The lower rows list representations of these groups in $I\bar{4}2m$.

The representations in the same column are compatible in the following sense: Bloch functions that are basis functions of a representation D_i in the upper row can be unitarily transformed into the basis functions of the representation given below D_i.

(iii)   The notations of the representations are defined in Table 2 of Ref. [6] and Table A1, respectively.

Table A3. Representations of the Bloch functions at the points of symmetry in the space group $I\bar{4}2m = \Gamma_q^v D_{2d}^{11}$ (121) of all the energy bands of antiferromagnetic BaMn$_2$As$_2$ with symmetry-adapted and optimally localized Wannier functions centered at the Mn, As, and Ba atoms, respectively.

Mn	Mn($\frac{1}{4}\frac{3}{4}\frac{1}{2}$)	Mn($\frac{3}{4}\frac{1}{4}\frac{1}{2}$)	KI	Γ	P	Z	X	N
Band 1	d_1	d_1	OK	$\Gamma_1 + \Gamma_2$	P_5	$Z_3 + Z_4$	$X_2 + X_4$	$N_1 + N_2$
Band 2	d_2	d_4	OK	Γ_5	$P_3 + P_4$	Z_5	$X_1 + X_3$	$N_1 + N_2$
Band 3	d_3	d_3	OK	$\Gamma_3 + \Gamma_4$	P_5	$Z_1 + Z_2$	$X_2 + X_4$	$N_1 + N_2$
Band 4	d_4	d_2	OK	Γ_5	$P_1 + P_2$	Z_5	$X_1 + X_3$	$N_1 + N_2$

As	As($zz0$)	As($\bar{z}\bar{z}0$)	KI	Γ	P	Z	X	N
Band 1	d_1	d_1	OK	$\Gamma_1 + \Gamma_4$	$P_1 + P_4$	$Z_1 + Z_4$	$2X_1$	$N_1 + N_2$
Band 2	d_2	d_2	OK	$\Gamma_2 + \Gamma_3$	$P_2 + P_3$	$Z_2 + Z_3$	$2X_3$	$N_1 + N_2$
Band 3	d_3	d_4	$-$	Γ_5	P_5	Z_5	$X_2 + X_4$	$N_1 + N_2$

Ba	Ba(000)	KI	Γ	P	Z	X	N
Band 1	d_1	OK	Γ_1	P_1	Z_1	X_1	N_1
Band 2	d_2	OK	Γ_2	P_2	Z_2	X_3	N_2
Band 3	d_3	OK	Γ_3	P_3	Z_3	X_3	N_1
Band 4	d_4	OK	Γ_4	P_4	Z_4	X_1	N_2

Notes to Table A3

(i) $z = 0.36\ldots$ [1]; the exact value of z is meaningless in this table.

(ii)   The antiferromagnetic structure of undistorted BaMn$_2$As$_2$ has the space group $I\bar{4}2m$ and the magnetic group $M = I\bar{4}2m + \{KI|000\}I\bar{4}2m$ with K denoting the operator of time-inversion.

(iii)   Each row defines a band with Bloch functions that can be unitarily transformed into Wannier functions being

- as well localized as possible;
- centered at the stated atoms;
- and symmetry-adapted to the space group $I\bar{4}2m$ of the antiferromagnetic structure in undistorted BaMn$_2$As$_2$.

(iv)   The notations of the representations are defined in Table A1.

(v)   The bands are determined following Theorem 5 of Ref. [5].

(vi)   The Wannier functions at the Mn, As or Ba atom listed in the upper row belong to the representation d_i included below the atom.

(vii)   The d_i denote the one-dimensional representations of the "point groups of the positions" of the Mn, As and Ba atom (Definition 12 of Ref. [5]), S_4, C_{2v}, and D_{2d}, respectively, defined by

Mn atoms	E	S_{4z}^+	C_{2z}	S_{4z}^-
d_1	1	1	1	1
d_2	1	i	-1	$-$i
d_3	1	-1	1	-1
d_4	1	$-$i	-1	i

As atoms	E	C_{2z}	σ_{da}	σ_{db}
d_1	1	1	1	1
d_2	1	1	-1	-1
d_3	1	-1	1	-1
d_4	1	-1	-1	1

Ba atom	E	C_{2z}	S_{4z}^- / S_{4z}^+	C_{2y} / C_{2x}	σ_{da} / σ_{db}
d_1	1	1	1	1	1
d_2	1	1	1	-1	-1
d_3	1	1	-1	1	-1
d_4	1	1	-1	-1	1

.

Notes to Table A3 (continued)

(viii) The entry "OK" indicates whether the Wannier functions may even be chosen symmetry-adapted to the magnetic group $M = I\bar{4}2m + \{KI|000\}I\bar{4}2m$ of undistorted $BaMn_2As_2$ (see Theorem 7 of Ref. [5]).

(ix) Hence, all the listed bands except for band 3 of As form magnetic bands as defined by Definition 16 of Ref. [5].

(x) Each band consists of one or two branches (Definition 2 of Ref. [5]) depending on the number of the related atoms in the unit cell.

Table A4. Character tables of the irreducible representations of the tetragonal space group $P\bar{4}2_1c = \Gamma_q D_{2d}^4$ (114) of the experimentally observed [1] antiferromagnetic structure in distorted $BaMn_2As_2$.

					$\{S_{4z}^-\|000\}$	$\{C_{2y}\|\frac{1}{2}\frac{1}{2}\frac{1}{2}\}$	$\{\sigma_{da}\|\frac{1}{2}\frac{1}{2}\frac{1}{2}\}$
	K	$\{KI\|\frac{1}{2}\frac{1}{2}\frac{1}{2}\}$	$\{E\|000\}$	$\{C_{2z}\|000\}$	$\{S_{4z}^+\|000\}$	$\{C_{2x}\|\frac{1}{2}\frac{1}{2}\frac{1}{2}\}$	$\{\sigma_{db}\|\frac{1}{2}\frac{1}{2}\frac{1}{2}\}$
Γ_1	(a)	(a)	1	1	1	1	1
Γ_2	(a)	(a)	1	1	1	−1	−1
Γ_3	(a)	(a)	1	1	−1	1	−1
Γ_4	(a)	(a)	1	1	−1	−1	1
Γ_5	(a)	(a)	2	−2	0	0	0

Table heading: $\Gamma(000)$

	K	$\{KI\|\frac{1}{2}\frac{1}{2}\frac{1}{2}\}$	$\{E\|000\}$	$\{C_{2z}\|010\}$	$\{C_{2z}\|000\}$	$\{E\|010\}$
M_1	(c)	(a)	1	1	−1	−1
M_2	(c)	(a)	1	1	−1	−1
M_3	(c)	(a)	1	1	−1	−1
M_4	(c)	(a)	1	1	−1	−1
M_5	(a)	(a)	2	−2	2	−2

Table heading: $M(\frac{1}{2}\frac{1}{2}0)$

	$\{\sigma_{da}\|\frac{1}{2}\frac{3}{2}\frac{1}{2}\}$	$\{\sigma_{db}\|\frac{1}{2}\frac{3}{2}\frac{1}{2}\}$	$\{S_{4z}^-\|010\}$	$\{S_{4z}^+\|010\}$	$\{C_{2x}\|\frac{1}{2}\frac{1}{2}\frac{1}{2}\}$	$\{C_{2y}\|\frac{1}{2}\frac{1}{2}\frac{1}{2}\}$
	$\{\sigma_{db}\|\frac{1}{2}\frac{1}{2}\frac{1}{2}\}$	$\{\sigma_{da}\|\frac{1}{2}\frac{1}{2}\frac{1}{2}\}$	$\{S_{4z}^+\|000\}$	$\{S_{4z}^-\|000\}$	$\{C_{2y}\|\frac{1}{2}\frac{3}{2}\frac{1}{2}\}$	$\{C_{2x}\|\frac{1}{2}\frac{3}{2}\frac{1}{2}\}$
M_1	1	−1	i	−i	i	−i
M_2	1	−1	−i	i	−i	i
M_3	−1	1	−i	i	i	−i
M_4	−1	1	i	−i	−i	i
M_5	0	0	0	0	0	0

Table heading: $M(\frac{1}{2}\frac{1}{2}0)$ (*continued*)

	K	$\{KI\|\frac{1}{2}\frac{1}{2}\frac{1}{2}\}$	$\{E\|000\}$	$\{C_{2z}\|001\}$	$\{C_{2z}\|000\}$	$\{E\|001\}$
Z_1	(c)	(a)	1	1	−1	−1
Z_2	(c)	(a)	1	1	−1	−1
Z_3	(c)	(a)	1	1	−1	−1
Z_4	(c)	(a)	1	1	−1	−1
Z_5	(a)	(a)	2	−2	2	−2

Table heading: $Z(00\frac{1}{2})$

Table A4. *Cont.*

	$Z(00\frac{1}{2})$ (*continued*)				
$\{C_{2y}\|\frac{1}{2}\frac{1}{2}\frac{3}{2}\}$	$\{C_{2x}\|\frac{1}{2}\frac{1}{2}\frac{3}{2}\}$	$\{S_{4z}^-\|001\}$	$\{S_{4z}^+\|001\}$	$\{\sigma_{da}\|\frac{1}{2}\frac{1}{2}\frac{1}{2}\}$	$\{\sigma_{db}\|\frac{1}{2}\frac{1}{2}\frac{1}{2}\}$
$\{C_{2x}\|\frac{1}{2}\frac{1}{2}\frac{1}{2}\}$	$\{C_{2y}\|\frac{1}{2}\frac{1}{2}\frac{1}{2}\}$	$\{S_{4z}^+\|000\}$	$\{S_{4z}^-\|000\}$	$\{\sigma_{db}\|\frac{1}{2}\frac{1}{2}\frac{3}{2}\}$	$\{\sigma_{da}\|\frac{1}{2}\frac{1}{2}\frac{3}{2}\}$
Z_1	1	-1	i	$-i$	i	$-i$
Z_2	1	-1	$-i$	i	$-i$	i
Z_3	-1	1	$-i$	i	i	$-i$
Z_4	-1	1	i	$-i$	$-i$	i
Z_5	0	0	0	0	0	0

		$A(\frac{1}{2}\frac{1}{2}\frac{1}{2})$			
	K	$\{KI\|\frac{1}{2}\frac{1}{2}\frac{1}{2}\}$	$\{E\|000\}$	$\{C_{2z}\|000\}$	$\{E\|001\}$	$\{C_{2z}\|001\}$
A_1	(c)	(a)	1	1	-1	-1
A_2	(c)	(a)	1	1	-1	-1
A_3	(c)	(a)	1	1	-1	-1
A_4	(c)	(a)	1	1	-1	-1
A_5	(b)	(a)	2	-2	-2	2

	$A(\frac{1}{2}\frac{1}{2}\frac{1}{2})$ (*continued*)				
$\{S_{4z}^-\|000\}$	$\{S_{4z}^-\|001\}$	$\{\sigma_{da}\|\frac{1}{2}\frac{1}{2}\frac{1}{2}\}$	$\{C_{2x}\|\frac{1}{2}\frac{1}{2}\frac{1}{2}\}$	$\{\sigma_{da}\|\frac{1}{2}\frac{1}{2}\frac{3}{2}\}$	$\{C_{2x}\|\frac{1}{2}\frac{1}{2}\frac{3}{2}\}$
$\{S_{4z}^+\|000\}$	$\{S_{4z}^+\|001\}$	$\{\sigma_{db}\|\frac{1}{2}\frac{1}{2}\frac{1}{2}\}$	$\{C_{2y}\|\frac{1}{2}\frac{1}{2}\frac{1}{2}\}$	$\{\sigma_{db}\|\frac{1}{2}\frac{1}{2}\frac{3}{2}\}$	$\{C_{2y}\|\frac{1}{2}\frac{1}{2}\frac{3}{2}\}$
A_1	-1	1	i	$-i$	$-i$	i
A_2	-1	1	$-i$	i	i	$-i$
A_3	1	-1	$-i$	$-i$	i	i
A_4	1	-1	i	i	$-i$	$-i$
A_5	0	0	0	0	0	0

		$R(0\frac{1}{2}\frac{1}{2})$			
			$\{C_{2y}\|\frac{1}{2}\frac{1}{2}\frac{3}{2}\}$	$\{C_{2z}\|001\}$	$\{C_{2x}\|\frac{1}{2}\frac{1}{2}\frac{3}{2}\}$
	$\{E\|000\}$	$\{E\|001\}$	$\{C_{2y}\|\frac{1}{2}\frac{1}{2}\frac{1}{2}\}$	$\{C_{2z}\|000\}$	$\{C_{2x}\|\frac{1}{2}\frac{1}{2}\frac{1}{2}\}$
R_1	2	-2	0	0	0

		$X(0\frac{1}{2}0)$			
			$\{C_{2y}\|\frac{1}{2}\frac{3}{2}\frac{1}{2}\}$	$\{C_{2z}\|010\}$	$\{C_{2x}\|\frac{1}{2}\frac{3}{2}\frac{1}{2}\}$
	$\{E\|000\}$	$\{E\|010\}$	$\{C_{2y}\|\frac{1}{2}\frac{1}{2}\frac{1}{2}\}$	$\{C_{2z}\|000\}$	$\{C_{2x}\|\frac{1}{2}\frac{1}{2}\frac{1}{2}\}$
X_1	2	-2	0	0	0

Notes to Table A4

(i)　The notations of the points of symmetry follow Figure 3.9 of Ref. [11].

(ii)　The character tables are determined from Table 5.7 of Ref. [11].

(iii)　K denotes the operator of time inversion. The entries (a), (b) and (c) indicate whether the related co-representations of the magnetic groups $P\overline{4}2_1c + \{K|000\}P\overline{4}2_1c$ and $P\overline{4}2_1c + \{KI|\frac{1}{2}\frac{1}{2}\frac{1}{2}\}P\overline{4}2_1c$ follow case (a), (b) or (c) as defined in Equations (7.3.45), (7.3.46) and (7.3.47), respectively, of Ref. [11] (and determined by Equation (7.3.51) of Ref. [11]). This information is interesting only in symmetry points invariant under the complete space group.

(iv)　The entries (a) and (c) for K and $\{KI|\frac{1}{2}\frac{1}{2}\frac{1}{2}\}$ show that all the one-dimensional representations at M, Z, or A are possible representations of a stable antiferromagnetic state (see Theorem 1 of Ref. [6] or Section III C of Ref. [15]).

Table A5. Compatibility relations between the Brillouin zone for the space group $I4/mmm$ (139) of tetragonal paramagnetic $BaMn_2As_2$ and the Brillouin zone for the space group $P\bar{4}2_1c$ (114) of the antiferromagnetic structure in distorted $BaMn_2As_2$.

$\Gamma(000)$									
Γ_1^+	Γ_2^+	Γ_3^+	Γ_4^+	Γ_5^+	Γ_1^-	Γ_2^-	Γ_3^-	Γ_4^-	Γ_5^-
Γ_1	Γ_2	Γ_3	Γ_4	Γ_5	Γ_3	Γ_4	Γ_1	Γ_2	Γ_5

$X(00\tfrac{1}{2})$							
X_1^+	X_2^+	X_3^+	X_4^+	X_1^-	X_2^-	X_3^-	X_4^-
M_5	$M_1 + M_2$	M_5	$M_3 + M_4$	M_5	$M_3 + M_4$	M_5	$M_1 + M_2$

$Z(\tfrac{1}{2}\tfrac{1}{2}\bar{\tfrac{1}{2}})$									
Z_1^+	Z_2^+	Z_3^+	Z_4^+	Z_5^+	Z_1^-	Z_2^-	Z_3^-	Z_4^-	Z_5^-
Γ_2	Γ_1	Γ_4	Γ_3	Γ_5	Γ_4	Γ_3	Γ_2	Γ_1	Γ_5

$P(\tfrac{1}{4}\tfrac{1}{4}\tfrac{1}{4})$				
P_1	P_2	P_3	P_4	P_5
$A_3 + A_4$	$A_3 + A_4$	$A_1 + A_2$	$A_1 + A_2$	$2A_5$

$\Lambda_M(\tfrac{1}{4}\tfrac{1}{4}\bar{\tfrac{1}{4}})$				line Λ
Λ_1	Λ_2	Λ_3	Λ_4	Λ_5
Z_5	Z_5	Z_5	Z_5	$Z_1 + Z_2 + Z_3 + Z_4$

Notes to Table A5

(i)　The Brillouin zone for $P\bar{4}2_1c$ lies within the Brillouin zone for $I4/mmm$.

(ii)　The upper rows list the representations of the little groups of the points of symmetry in the Brillouin zone for $I4/mmm$, and the lower rows list representations of the little groups of the related points of symmetry in the Brillouin zone for $P\bar{4}2_1c$.

　　The representations in the same column are compatible in the following sense: Bloch functions that are basis functions of a representation D_i in the upper row can be unitarily transformed into the basis functions of the representation given below D_i.

(iii)　The notations of the representations are defined in Table 2 of Ref. [6] and Table A4, respectively.

(iv)　$\Lambda_M(\tfrac{1}{4}\tfrac{1}{4}\bar{\tfrac{1}{4}})$ denotes the midpoint between Γ and Z in the Brillouin zone for $I4/mmm$.

(v)　The representations on the line Λ in the Brillouin zone for $I4/mmm$ are simple: the branch connecting Γ_5 and Z_5 in Figure 2 is labeled by the two-dimensional representation Λ_5, all the other branches are labeled by one of the one-dimensional representations Λ_1, Λ_2, Λ_3, or Λ_4.

(vi)　The compatibility relations are determined in the way described in great detail in Ref. [7].

Table A6. Representations of the Bloch functions at the points of symmetry in the space group $P\bar{4}2_1c$ (114) of all the energy bands of *distorted* antiferromagnetic $BaMn_2As_2$ with symmetry-adapted and optimally localized Wannier functions centered at the Mn, As, or Ba atoms, respectively.

Mn	$Mn(\tfrac{1}{2}0\tfrac{1}{4})$	$Mn(0\tfrac{1}{2}\tfrac{1}{4})$	$Mn(1\tfrac{1}{2}\tfrac{3}{4})$	$Mn(\tfrac{1}{2}1\tfrac{3}{4})$	$\{KI\|\tfrac{1}{2}\tfrac{1}{2}\tfrac{1}{2}\}$	Γ
Band 1	d_1	d_1	d_1	d_1	OK	$\Gamma_1 + \Gamma_2 + \Gamma_3 + \Gamma_4$
Band 2	d_2	d_2	d_2	d_2	$*$	$2\Gamma_5$

(*continued*)					
Mn	M	Z	A	R	X
Band 1	$M_1 + M_2 + M_3 + M_4$	$2Z_5$	$2A_5$	$2R_1$	$2X_1$
Band 2	$2M_5$	$Z_1 + Z_2 + Z_3 + Z_4$	$A_1 + A_2 + A_3 + A_4$	$2R_1$	$2X_1$

Table A6. *Cont.*

As	As(00z)	As(00z̄)	As($\frac{1}{2}\frac{1}{2},\frac{1}{2}+z$)	As($\frac{1}{2}\frac{1}{2},\frac{1}{2}-z$)	$\{KI|\frac{1}{2}\frac{1}{2}\frac{1}{2}\}$	Γ
Band 1	d_1	d_1	d_1	d_1	OK	$\Gamma_1 + \Gamma_2 + \Gamma_3 + \Gamma_4$
Band 2	d_2	d_2	d_2	d_2	*	$2\Gamma_5$

			(continued)				
As	**M**		**Z**		**A**	**R**	**X**
Band 1	$2M_5$		$2Z_5$		$A_1 + A_2 + A_3 + A_4$	$2R_1$	$2X_1$
Band 2	$M_1 + M_2 + M_3 + M_4$		$Z_1 + Z_2 + Z_3 + Z_4$		$2A_5$	$2R_1$	$2X_1$

Ba	Ba(000)	Ba($\frac{1}{2}\frac{1}{2}\frac{1}{2}$)	$\{KI|\frac{1}{2}\frac{1}{2}\frac{1}{2}\}$	Γ	**M**	**Z**	**A**	**R**	**X**
Band 1	d_1	d_1	OK	$\Gamma_1 + \Gamma_2$	M_5	Z_5	$A_3 + A_4$	R_1	X_1
Band 2	d_2	d_4	OK	Γ_5	$M_1 + M_4$	$Z_1 + Z_4$	A_5	R_1	X_1
Band 3	d_3	d_3	OK	$\Gamma_3 + \Gamma_4$	M_5	Z_5	$A_1 + A_2$	R_1	X_1
Band 4	d_4	d_2	OK	Γ_5	$M_2 + M_3$	$Z_2 + Z_3$	A_5	R_1	X_1

Notes to Table A6

(i) $z = 0.36\ldots$ [1]; the exact value of z is meaningless in this table.

(ii)   The space group $P\bar{4}2_1c$ leaves invariant the experimentally observed [1] antiferromagnetic structure and defines the distortion of BaMn$_2$As$_2$ that possesses the magnetic super band consisting of band 1 of Mn, band 2 of As, and band 3 of Ba.

(iii)   The appertaining magnetic group reads as $M = P\bar{4}2_1c + \{KI|\frac{1}{2}\frac{1}{2}\frac{1}{2}\}P\bar{4}2_1c$, where K still denotes the operator of time-inversion.

(iv)   The notations of the representations are defined in Table A4.

(v)   The bands are determined following Theorem 5 of Ref. [5].

(vi)   Each row defines a band with Bloch functions that can be unitarily transformed into Wannier functions being

- as well localized as possible;
- centered at the stated atoms; and
- symmetry-adapted to $P\bar{4}2_1c$.

(vii)   The Wannier functions at the Mn, As or Ba atom listed in the upper row belong to the representation d_i included below the atom.

(viii)   The d_i denote the representations of the "point groups of the positions" of the Mn, As and Ba atoms (Definition 12 of Ref. [5]), C_2, C_2, and S_4, respectively, defined by

Mn Atoms		
	$\{E|000\}$	$\{C_{2z}|000\}$
d_1	1	1
d_2	1	−1

As Atoms		
	$\{E|000\}$	$\{C_{2z}|000\}$
d_1	1	1
d_2	1	−1

Ba Atoms				
	$\{E|000\}$	$\{S_{4z}^{+}|000\}$	$\{C_{2z}|000\}$	$\{S_{4z}^{-}|000\}$
d_1	1	1	1	1
d_2	1	i	−1	−i
d_3	1	−1	1	−1
d_4	1	−i	−1	i

.

Notes to Table A6 (continued)

(ix) The entry "OK" indicates whether the Wannier functions may even be chosen symmetry-adapted to the magnetic group $M = P\bar{4}2_1c + \{KI|\frac{1}{2}\frac{1}{2}\frac{1}{2}\}P\bar{4}2_1c$ (see Theorem 7 of Ref. [5]).

(x) The asterisk "$*$" indicates that the Wannier functions may be chosen symmetry-adapted to the magnetic group M, but they do not allow that the magnetic moments are situated at the appertaining atoms. This complication (which has not yet been considered in Ref. [5]) may (but does not necessarily) occur only if the representations of the space group at point Γ are not one-dimensional, as it is the case in band 2 of both Mn and As, and in bands 2 and 4 of Ba. Consider, for example, band 2 of Mn and the two $Mn(\frac{1}{2}0\frac{1}{4})$ and $Mn(\frac{1}{2}1\frac{3}{4})$ atoms. The magnetic moments at the two positions A and B of these atoms are anti-parallel. Thus, the two Wannier functions $w_A(\vec{r})$ and $w_B(\vec{r})$ at these positions are complex conjugate, $w_A(\vec{r}) = w_B^*(\vec{r})$, and, hence, belong to co-representations d_A and d_B of the groups of these positions being also complex conjugate,

$$d_A = d_B^*. \tag{8}$$

The matrix $\mathbf{N}$ defined by Theorem 7 of Ref. [5] takes the form $\mathbf{N} = \begin{pmatrix} 0 & 1 & 0 & 0 \\ 1 & 0 & 0 & 0 \\ 0 & 0 & 0 & 1 \\ 0 & 0 & 1 & 0 \end{pmatrix}$ in band 2 of Mn, yielding the two co-representations d_A and d_B,

	E	C_{2z}	$K\sigma_x$	$K\sigma_y$
d_A	1	-1	1	-1
d_B	1	-1	-1	1

.

Because d_A and d_B do not comply with Equation (8), the Wannier functions defined by band 2 of Mn do not form a magnetic band in antiferromagnetic $BaMn_2As_2$ since it is experimentally proven that the ordered magnetic moments lie at the Mn atoms. The Wannier functions defined by band 2 of As, on the other hand, form a magnetic band in $BaMn_2As_2$ because the As atoms do not bear ordered magnetic moments.

(xi) Each band consists of two or four branches (Definition 2 of Ref. [5]) depending on the number of the related atoms in the unit cell.

Table A7. Character tables of the single-valued irreducible representations of the tetragonal space group $P\bar{4} = \Gamma_q S_4^1$ (81).

		$\Gamma(000)$, $M(\frac{1}{2}\frac{1}{2}0)$, $Z(00\frac{1}{2})$, $A(\frac{1}{2}\frac{1}{2}\frac{1}{2})$			
	K	KC_{2a}	E	S_{4z}^+	C_{2z}	S_{4z}^-
R_1	(a)	(a)	1	1	1	1
R_2	(c)	(a)	1	i	-1	$-i$
R_3	(a)	(a)	1	-1	1	-1
R_4	(c)	(a)	1	$-i$	-1	i

Notes to Table A7

(i) The notations of the points of symmetry follow Figure 3.9 of Ref. [11].

(ii) Only the points of symmetry invariant under the complete space group are listed.

(iii) The character tables are determined from Table 5.7 in Ref. [11].

(iv) K still denotes the operator of time inversion. The entries (a) and (c) indicate whether the related co-representations of the magnetic groups $P\bar{4} + \{K|000\}P\bar{4}$ and $P\bar{4} + \{KC_{2a}|000\}P\bar{4}$ follow case (a) or case (c) as defined in Equations (7.3.45) and (7.3.47), respectively, of Ref. [11] (and determined by Equation (7.3.51) of Ref. [11]).

(v) The entries (a) and (c) for K and KC_{2a} show that the representations R_2 and R_4 at any of the points Γ, M, Z, or A are possible representations of a stable antiferromagnetic state (see Theorem 1 of Ref. [6] or Section III C of Ref. [15]). This is important since M_{81} (6) is the *exact* group of the magnetic structure in $BaMn_2As_2$.

References

1. Singh, Y.; Green, M.A.; Huang, Q.; Kreyssig, A.; McQueeney, R.J.; Johnston, D.C.; Goldman, A.I. Magnetic order in $BaMn_2As_2$ from neutron diffraction measurements. *Phys. Rev. B* **2009**, *80*, doi:10.1103/PhysRevB.80.100403.

2. Huang, Q.; Qiu, Y.; Bao, W.; Green, M.A.; Lynn, J.W.; Gasparovic, Y.C.; Wu, T.; Wu, G.; Chen, X.H. Neutron-diffraction measurements of magnetic order and a structural transition in the parent $BaFe_2As_2$ compound of FeAs-based high-temperature superconductors. *Phys. Rev. Lett.* **2008**, *101*, doi:10.1103/PhysRevLett.101.257003.

3. An, J.; Sefat, A.S.; Singh, D.J.; Du, M.H. Electronic structure and magnetism in $BaMn_2As_2$ and $BaMn_2Sb_2$. *Phys. Rev. B* **2009**, *79*, doi:10.1103/PhysRevB.79.075120.

4. Singh, Y.; Ellern, A.; Johnston, D.C. Magnetic, transport, and thermal properties of single crystals of the layered arsenide $BaMn_2As_2$. *Phys. Rev. B* **2009**, *79*, doi:10.1103/PhysRevB.79.094519.

5. Krüger, E.; Strunk, H.P. Group theory of wannier functions providing the basis for a deeper understanding of magnetism and superconductivity. *Symmetry* **2015**, *7*, 561–598.

6. Krüger, E.; Strunk, H.P. Structural distortion in antiferromagnetic $BaFe_2As_2$ as a result of time-inversion symmetry. *J. Supercond.* **2014**, *27*, 601–612.

7. Krüger, E. Symmetry of Bloch functions in the space group D_{4h}^6 of perfect antiferromagnetic chromium. *Phys. Rev. B* **1985**, *32*, 7493–7501.

8. Krüger, E. Nonadiabatic extension of the Heisenberg model. *Phys. Rev. B* **2001**, *63*, doi:10.1103/PhysRevB.63.144403.

9. Mott, N.F. On the transition to metallic conduction in semiconductors. *Can. J. Phys.* **1956**, *34*, 1356–1368.

10. Hubbard, J. Elelectron correlations in narrow energy bands. *Proc. R. Soc. London Ser. A* **1963**, *276*, 238–257.

11. Bradley, C.; Cracknell, A.P. *The Mathematical Theory of Symmetry in Solids*; Claredon: Oxford, UK, 1972.

12. Krüger, E.; Strunk, H.P. The structural distortion in antiferromagnetic LaFeAsO investigated by a group-theoretical approach. *J. Supercond.* **2011**, *24*, 2103–2117.

13. Blum, V.; Gehrke, R.; Hanke, F.; Havu, P.; Havu, V.; Ren, X.; Reuter, K.; Scheffler, M. Ab initio molecular simulations with numeric atom-centered orbitals. *Comput. Phys. Commun.* **2009**, *180*, 2175–2196.

14. Havu, V.; Blum, V.; Havu, P.; Scheffler, M. Efficient $O(N)$ integration for all-electron electronic structure calculation using numeric basis functions. *Comput. Phys. Commun.* **2009**, *228*, 8367–8379.

15. Krüger, E. Stability and symmetry of the spin-density-wave-state in chromium. *Phys. Rev. B* **1989**, *40*, 11090–11103.

16. Krüger, E. Energy band with Wannier functions of ferromagnetic symmetry as the cause of ferromagnetism in iron. *Phys. Rev. B* **1999**, *59*, 13795–13805.

17. De la Cruz, C.; Huang, Q.; Lynn, J.W.; Li, J.; Ratcliff, W., II; Zarestky, J.L.; Mook, H.A.; Chen, G.F.; Luo, J.L.; Wang, N.L.; et al. Magnetic order close to superconductivity in the iron-based layered $LaO_{1-x}F_xFeAs$ systems. *Nature* **2008**, *453*, 899–902.